09,04

The evolution of the spectral and structural characteristics of $La_{0.98-x}Lu_xEu_{0.02}BO_3$ orthoborates

© S.Z. Shmurak, V.V. Kedrov, A.P. Kiselev, T.N. Fursova, I.I. Zver'kova, S.S. Khasanov

Osipyan Institute of Solid State Physics RAS,
Chernogolovka, Russia

E-mail: shmurak@issp.ac.ru

Received July 21, 2021
Revised July 21, 2021
Accepted July 23, 2021

The structure, IR absorption, luminescence, and luminescence excitation spectra of $La_{0.98-x}Lu_xEu_{0.02}BO_3$ orthoborates synthesized at 970°C were studied at $0 \le x \le 0.98$. An increase in x leads to a sequential change of the structural state of the orthoborates. At first, the compound has the aragonite structure. Then, it becomes two-phase and contains the aragonite and vaterite phases. With a further increase in x, the compounds have the vaterite structure, then the vaterite and calcite structure, and, finally, the calcite structure. Correspondence between the structure and spectral characteristics of these compounds was established. Luminescence spectra were investigated at different wavelengths of exciting light. This allowed obtaining information on the structure of a near-surface layer and the bulk of microcrystals of the investigated samples. It is shown that the vaterite phase arises in the bulk of microcrystals of samples that have the aragonite structure.

Keywords: phosphors for LEDs, rare earth orthoborates, X-ray diffraction analysis, IR spectroscopy, luminescence spectra.

DOI: 10.21883/PSS.2022.14.54342.172

1. Introduction

In recent years the large number of works is dedicated to studies of spectral and structural characteristics of molybdates, tungstates, garnets and borates, alloyed with rare earth element ions. Interest to these compounds is related to the fact, that they are efficient luminophores and can be used in LED light sources [1–11]. To obtain various shades of „white" light it is very important to directionally control the spectral characteristics of luminophores. One of the most efficient methods of directional modification of polymorphous luminophores radiation spectrum is to change their structural state, since each structural modification of molybdates, tungstates and borates, containing optical active centers, corresponds to specific and unique luminescence spectrum (LS). For instance, in luminescence spectrum of calcite modification of $LuBO_3$(Eu) two narrow bands with $\lambda_{max} \sim 590$ and 596 nm are observed, while LS of vaterite structure of $LuBO_3$(Eu) contains several lines, grouped in three bands in wavelength region of 593, 611 and 628 nm [1–3,12,13]. Therefore, the orange luminescence is characteristic for the calcite modification of $LuBO_3$(Eu) and red luminescence — for the vaterite structure.

Significant modifications of luminescence spectra of Eu^{3+} ions at luminophore structure change allow to use Eu^{3+} ions as structure-sensitive and optically active markers for identification of structural state of rare earth element borates. As known, rare earth ions — RE^{3+} (including Eu^{3+}) are sensitive to the closest surrounding [14,15]. Therefore, the change of spectral characteristics of RE^{3+} ions allows to evaluate the change of their local surrounding. Eu^{3+} ions allow to monitor the structural state both in volume and on surface of a sample. Information on the closest surrounding of Eu^{3+} ions in crystal volume can be observed by excitation of luminescence of Eu^{3+} ions with a light with energy, corresponding to resonance excitation of ions of Eu^{3+} ($\lambda_{ex} \sim 394$ and ~ 466 nm, electron transition of $^7F_0 \rightarrow {}^5L_6$ and $^7F_0 \rightarrow {}^5D_2$ respectively), in transparent region of a crystal ($\lambda > 300$ nm) [1–3,12,13].

Excitation of rare earth ions luminescence with a light with energy within intense absorption region of a sample ($\lambda = 225-300$ nm), charge transfer band (CTB), allows to obtain information on local surrounding of Eu^{3+} ions in near-surface crystal layer [1–3,12,13].

In the works [6–8] it is shown, that if the closest order surround Eu^{3+} ions is the same for the whole sample, that is indicated by correspondence of luminescence spectra (LS) of near-surface sample layer and its volume, the sample is single-phase.

Lutetium orthoborate has two stable structural modifications: vaterite, that is formed during $LuBO_3$ synthesis at $T = 750-850$°C, and calcite, formed at $T = 970-1100$°C. The lutetium ion in calcite and vaterite structures is surrounded by six and eight oxygen atoms respectively. Orthoborates of $REBO_3$ (RE = Eu, Gd, Tb, Dy, Y) and $InBO_3$ have different, but only one structural modification: vaterite for the mentioned orthoborates of rare earth elements and calcite for indium orthoborate [16–21]. Solid solution of $Lu_{1-x}In_xBO_3$, synthesized at 780°C ($LuBO_3$ vaterite presence temperature), is crystallized in calcite structure at $x > 0.08-0.1$ [22]. At the same time, solid

solutions of $Lu_{1-x}RE_xBO_3$ (RE = Eu, Gd, Tb, Dy and Y) at $x > 0.15-0.2$, synthesized at $T = 970-1100°C$ ($LuBO_3$ calcite phase presence temperature), are crystallized at vaterite structure [12,13].

Luminescence studies of $Lu_{0.98-x}In_xEu_{0.02}BO_3$ compounds at excitation in charge transfer band ($\lambda_{ex} = 250$ nm) and at resonance excitation of Eu^{3+} ions ($\lambda_{ex} = 394$ nm) showed, that structural transformations in orthoborates of $Lu_{0.98-x}In_xEu_{0.02}BO_3$ at In^{3+} ions concentration increase begin in near-surface layer of these samples microcrystals [22]. At $x \geq 0.04$ the near-surface layer has calcite structure, with the further increase of indium concentration the amount of calcite phase also increases in sample volume, and at $x > 0.1$ the whole sample has calcite structure.

Study of orthoborates of $Lu_{0.99-x}RE_xEu_{0.01}BO_3$ (RE = Gd, Eu, Tb, Y), synthesized at 970°C, showed, that with RE concentration increase the changes of their structure are observed: at $0 \leq x \leq 0.05-0.1$ the solid solution of ortoborates is single-phase and has calcite structure (sp. gr. $R\bar{3}c$); at $0.05-0.1 < x \leq 0.1-0.25$ along with calcite structure the vaterite phase appears (sp. gr. $C2/c$), and at $x > 0.1-0.25$ the solid solution is single-phase with vaterite structure (sp. gr. $C2/c$) [23,24]. Morphology of orthoborate microcrystals changes simultaneously with the structure. Microcrystals of calcite modification are large with particles size of $15-20\,\mu$m. Small microcrystals ($1-2\,\mu$m), number of which increases with increase of x, form (along with large ones) in RE concentration interval of $0.05-0.1 < x \leq 0.1-0.25$, where the samples are two-phase. With $x > 0.1-0.25$ there are mainly microcrystals sized $1-2\,\mu$m with a vaterite structure. It is important to note, that vaterite phase appears in volume of large microcrystals with calcite structure, and with the further increase of RE ions concentration the vaterite phase is also observed on their surface.

Thus, the calcite formation in microcrystals of $Lu_{0.98-x}In_xEu_{0.02}BO_3$, with initial vaterite structure, at In^{3+} concentration increase happens initially in near-surface sample regions, while vaterite formation in initial large microcrystals of $Lu_{0.99-x}RE_xEu_{0.01}BO_3$, with calcite structure, happens at RE^{3+} concentration increase initially in these microcrystals volume.

It is important to note, that the works [12,13,22–24] were dedicated to the study of solid solutions of lutetium borate, having two structural modifications (vaterite and calcite), and borates, having only one modification of lutetium borate: either calcite ($InBO_3$) or vaterite ($REBO_3$, RE = Eu, Gd, Tb, Dy, Y). Study of structural state of solid solution of $LuBO_3$ and borate, which structure is neither calcite nor vaterite, is of interest. Lantanium ortoborate ($LaBO_3$) meets this condition and has two phase states: the low-temperature orthorhombic aragonite phase (sp. gr. $Pnam$) and the high-temperature monoclinic phase (sp. gr. $P2_1/m$), to which $LaBO_3$ transitions at 1488°C [17,25]. The works [26,27] demonstrate, that temperature sequences of structural states at solid-phase synthesis of $LaBO_3$ from amorphous and microcrystalline precursors are different. At $LaBO_3$ synthesis from microcrystalline powder the low-temperature phase of aragonite forms initially (at 900°C), and then — the high-temperature monoclinic phase. The following phase sequence is observed at synthesis from amorphous precursor: (high-temperature) monoclinic ($T = 500°C$), low-temperature orthorhombic phase of aragonite ($T = 800°C$), high-temperature monoclinic phase ($T = 1488°C$).

It should be noted, that unusual sequence of structural states change was observed earlier at annealing of amorphous samples of europium molybdate $Eu_2(MoO_4)_3$: amorphous state → (550°C) high-temperature β-phase (metastable under these conditions) → (700°C) α-phase (thermodynamically stable under these conditions) → (∼ 881°C) β-phase (thermodynamically stable until melting point) [28]. Luminescence study at various excitation wavelengths allowed to study the process of crystalline phases formation on surface and in volume of microcrystalline samples. At annealing of amorphous $Eu_2(MoO_4)_3$ the high-temperature β-phase nucleates at 500°C simultaneously in volume and on surface of microcrystals. At the same time, nucleation of α-phase, thermodynamically stable at $T \leq 881°C$, happens at ∼ 650°C in volume of microcrystals. At 850°C nucleation of β-phase happens in the whole sample, both in volume and on surface of microcrystals. The same sequence of structural states change is observed at annealing of amorphous $Gd_2(MoO_4)_3$(Eu) (Eu^{3+} ions were used as structure-sensitive and optically active markers). Moreover, as in europium molybdate, the formation of β-phase happens both in volume and on surface of microcrystals (in the whole sample volume), while α-phase — in volume of microcrystals [8].

Luminescence spectra (LS) and luminescence excitation spectra (LES) of orthoborates of $LaBO_3$(Eu), obtained using different methods and with different morphology, are studied in the works [26,29–31]. In luminescence spectra of $LaBO_3$(Eu) the bands, corresponding to transitions of $^5D_0 \rightarrow {}^7F_J$ ($J = 0, 1, 2, 3, 4$) in Eu^{3+} ions, are observed. Bands with $\lambda_{max} = 588-595$ nm ($^5D_0 \rightarrow {}^7F_1$) and $610-626$ nm ($^5D_0 \rightarrow {}^7F_2$) have the highest intensity. In luminescence excitation spectra the short-wave charge transfer band (CTB) of $\lambda_{ex} = 270-285$ nm has the highest intensity. In the long-wave region of the spectrum in a wavelength range of $300-430$ nm several bands are observed in LES due to $f \rightarrow f$-transitions in Eu^{3+} ion. The band with $\lambda_{ex} = 393-394$ nm ($^7F_0 \rightarrow {}^5L_6$) has the highest intensity.

Structure of $LaBO_3$ is studied in the works [27,29,31–34]. La^{3+} ions in the aragonite structure are surrounded by nine oxygen ions, while boron ions have a trigonal coordination by oxygen. It should be noted that Lu^{3+} ions in the calcite structure, e.g. in $LuBO_3$, are surrounded by six oxygen ions, while boron atoms have a trigonal coordination by oxygen, as in aragonite, — $(BO_3)^{3-}$ [35]. At the same time, Lu^{3+} ions in the vaterite structure are surrounded by eight

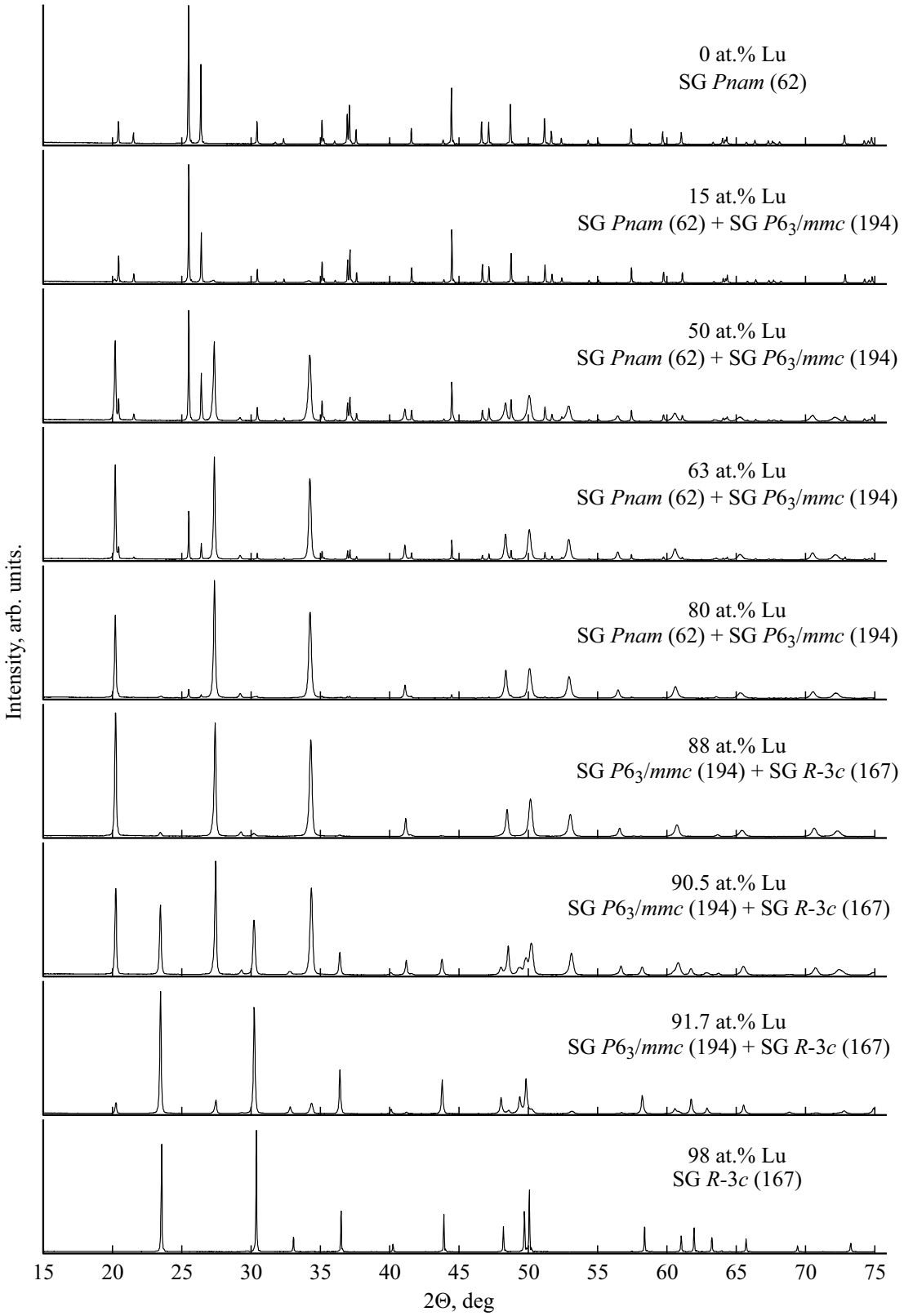

Figure 1. Diffractograms of samples $La_{0.98-x}Lu_xEu_{0.02}BO_3$ $(0 \leq x \leq 0.98)$.

oxygen ions, while three boron atoms with a tetrahedral environment by oxygen make up a group $(B_3O_9)^{9-}$ in the form of a three-dimensional ring [36,37].

In this work the studies of changes of structure, morphology, IR-spectra and spectra of luminescence excitation and luminescence of solid solutions of $La_{0.98-x}Lu_xEu_{0.02}BO_3$ in a wide range of concentrations of Lu ($0 \le x \le 0.98$) are presented. Eu^{3+} ions were used as optically active and structure-sensitive markers. The correspondence between structure and spectral characteristics of this compound is established. Compositions with maximum luminescence intensity of ions of Eu^{3+} in $La_{0.98-x}Lu_xEu_{0.02}BO_3$ are determined.

2. Experimental procedures

2.1. Sample synthesis

Samples of orthoborate polycrystalline powders with composition of $La_{0.98-x}Lu_xEu_{0.02}BO_3$ were obtained by interaction of oxides of rare earth elements with molten potassium tetraborate according to the reaction

$$(0.98-x)La_2O_3 + xLu_2O_3 + 0.02Eu_2O_3 + K_2B_4O_7 = 2La_{0.98-x}Lu_xEu_{0.02}BO_3 + K_2B_2O_4.$$

The potassium tetraborate amount taken for the reaction provided a 10–20% excess of the boron-containing reagent in relation to the stoichiometric amount. The initial compounds for orthoborates synthesis were tetrahydrate of potassium tetraborate $K_2B_4O_7 \cdot 4H_2O$ and oxides La_2O_3, Lu_2O_3, Eu_2O_3. All the used chemical substances were of „analytical reagent grade".

Microcrystalline orthoborate powders were synthesized as follows. Weighted stoichiometric amounts of REE oxides and tetrahydrate of potassium tetraborate were put into a ceramic cup, distilled water was added and everything was thoroughly mixed. The obtained aqueous suspension was heated on a hot plate and water was driven off under careful boiling. The obtained solid product was annealed at temperature of 600°C for 20 min to remove water, and then thoroughly ground in an agate mortar. The obtained powder was transferred into a ceramic crucible and subjected to high-temperature annealing at $T = 970$°C for 2 h. The annealing product was treated with aqueous solution of hydrochloric acid with the concentration of 5 wt.% for 0.2 h while constantly mixing. Orthoborate polycrystals were isolated by filtering the obtained aqueous suspension, followed by washing with water, alcohol, and product drying on a filter. The obtained powders of orthoborate polycrystals were finally dried in air at $T = 200$°C for 0.5 h.

2.2. Research methods

X-ray diffraction studies were performed using a Rigaku SmartLab SE diffractometer with CuK_α radiation, $\lambda = 1.54178$ Å, 40 kV, 35 mA. Angular interval $2\theta = 10-140°$. Phase analysis of the samples and calculation of lattice parameters were performed using the Match and PowderCell 2.4 programs.

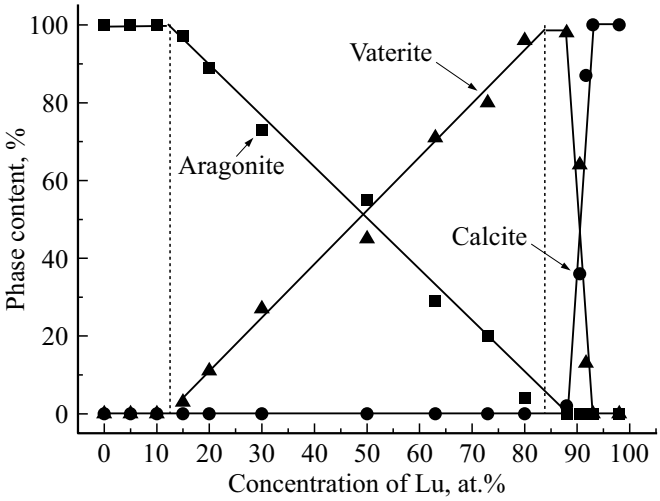

Figure 2. Phase composition of the synthesized samples of $La_{0.98-x}Lu_xEu_{0.02}BO_3$ depending on rare earths ratio in the charge at $0 \le x \le 0.98$: a square — aragonite, a triangle — vaterite, a circle — calcite.

Samples IR-spectra were measured in a VERTEX 80v Fourier-spectrometer in the spectral range of 400–5000 cm^{-1} with resolution of 2 cm^{-1}. For measurements, the polycrystal powders were ground in an agate mortar, and then were applied in a thin layer onto a crystalline polished substrate of KBr.

The samples morphology was studied using a Supra 50VP X-ray microanalyzer with an add-on for EDS INCA (Oxford).

Photoluminescence spectra and luminescence excitation spectra were studied on a unit that consisted of a light source — DKSSh-150 lamp, two MDR-4 and MDR-6 monochromators (spectral range is 200–1000 nm, dispersion is 1.3 nm/mm). Luminescence was recorded by means of FEU-106 photomultiplier (spectral sensitivity range is 200–800 nm) and an amplification system. The MDR-4 monochromator was used to study the samples luminescence excitation spectra, the MDR-6 monochromator was used to study luminescence spectra.

Spectral and structural characteristics, as well as samples morphology were studied at room temperature.

3. X-ray diffraction studies

Diffraction pattern of powder samples of the examined compounds of $La_{0.98-x}Lu_xEu_{0.02}BO_3$ and their phase composition at $0 \le x \le 0.98$ are presented in Figs 1 and 2. With Lu^{3+} concentration increase the sequential change of various types of structural modifications happens. At $0 \le x < 0.15$ the samples are single-phase and have aragonite structure, sp. gr. *Pnam* № 62 (PDF 12-0762), $Z = 4$. In a range

Table 1. Influence of Lu^{3+} concentration on content of aragonite, vaterite and calcite phases in orthoborates of $La_{0.98-x}Lu_xEu_{0.02}BO_3$

Concentration La^{3+}, at.%	Aragonite (PDF 12-0762), %	Volume of lattice aragonite cell, reduced to $Z = 2$, Å^3	Vaterite SG 194 (PDF 74-1938), %	Volume of lattice vaterite cell, $Z = 2$, Å^3	Calcite SG 167 (PDF-72-1053), %	Volume of lattice calcite cell, reduced to $Z = 2$, Å^3
0	100	123.6	0		0	
5	100	123.4	0		0	
10	100	123.3	0		0	
15	97	123.3	3		0	
20	89	123.3	11		0	
30	73	123.4	27	107.9	0	
50	55	123.3	45	107.7	0	
63	29	123.3	71	107.6	0	
73	20	123.1	80	107.6	0	
80	4		96	107.5	0	
88	0		98	107.1	2	
90.5	0		64	106.0	36	114.1
91.7	0		13	106.1	87	114.3
93	0		0		100	114.4
98	0		0		100	113.2
[1)]90	0		93		7	

Note. [1)] Sample of $La_{0.1}Lu_{0.9}BO_3$

of $0.15 \le x \le 0.80$ the samples are two-phase — along with aragonite structure the vaterite structure is observed, sp.gr. $P6_3/mmc$ № 194 (PDF 74-1938), $Z = 2$. At $0.88 \le x \le 0.98$ the aragonite phase in the samples is not observed. A calcite phase, sp.gr. $R\bar{3}c$ № 167 (PDF 72-1053), $Z = 6$, amount of which increases with increase of Lu^{3+} concentration, is observed in ortoborate with composition of $La_{0.10}Lu_{0.88}Eu_{0.02}BO_3$ along with the vaterite. At $0.88 \le x < 0.93$ the samples are two-phase — they contain vaterite and calcite phases. In concentrations range of $0.93 \le x \le 0.98$ the samples are single-phase with calcite structure.

At lutetium concentrations of $0 \le x < 0.15$ in a single-phase sample with aragonite structure the monotonous reduction of lattice cell volume at x increase is observed, indicating the lutetium dissolution in aragonite structure. At $x \ge 0.15$ the second phase (vaterite) appears in the sample, along with aragonite, while aragonite lattice cell volume remains constant. The excessive lutetium does not make part of the aragonite structure, but is consumed for increase of the vaterite phase amount.

In two-phase region of $0.15 \le x \le 0.80$ (aragonite + vaterite) the lattice cell volume of vaterite also does not change, indicating the composition consistency in vaterite structure. The approximate composition of the vaterite phase, estimated along the boundary of vaterite lattice cell volume change is $\sim La_{0.14}Lu_{0.84}Eu_{0.02}BO_3$. As seen from Fig. 2, the ratio of aragonite and vaterite phases changes in the concentration interval of Lu^{3+} $0.15 \le x \le 0.80$.

For samples with calcite structure at $0.93 \le x \le 0.98$ the lattice cell volume reduces with Lu^{3+} concentration increase. Consequently, when $Lu_{0.98}Eu_{0.02}BO_3$ is doped with La^{3+} ions in the concentration range of 0–5 at.%, the calcite lattice cell volume increases, indicating lantanium dissolution in the lutetium orthoborate with a calcite structure. In two-phase region (at $0.88 \le x < 0.93$) the volume of calcite lattice cell is constant, volume of vaterite lattice cell increases with lantanium concentration increase in the charge (i.e. reduces with lutetium content increase), the ratio between amount of phases of vaterite and calcite also changes (Table 1, Fig. 3)

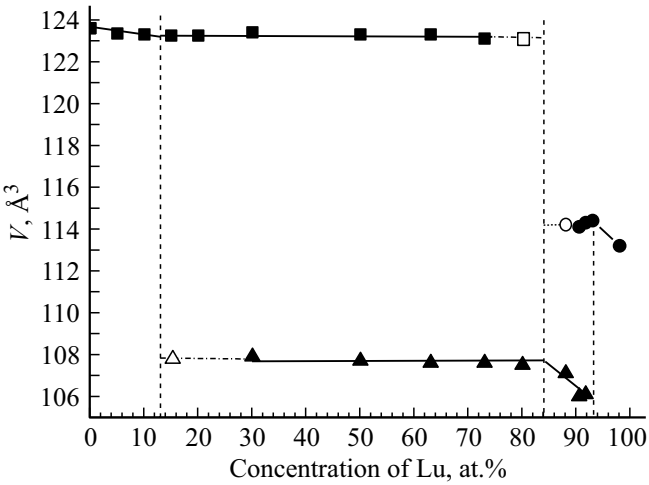

Figure 3. Volumes of lattice cells of structural modifications of $La_{0.98-x}Lu_xEu_{0.02}BO_3$ at $0 \le x \le 0.98$, reduced to $Z = 2$: a square — aragonite, a triangle — vaterite, a circle — calcite (assumed volume values: an empty square — aragonite, an empty triangle — vaterite, an empty circle — calcite).

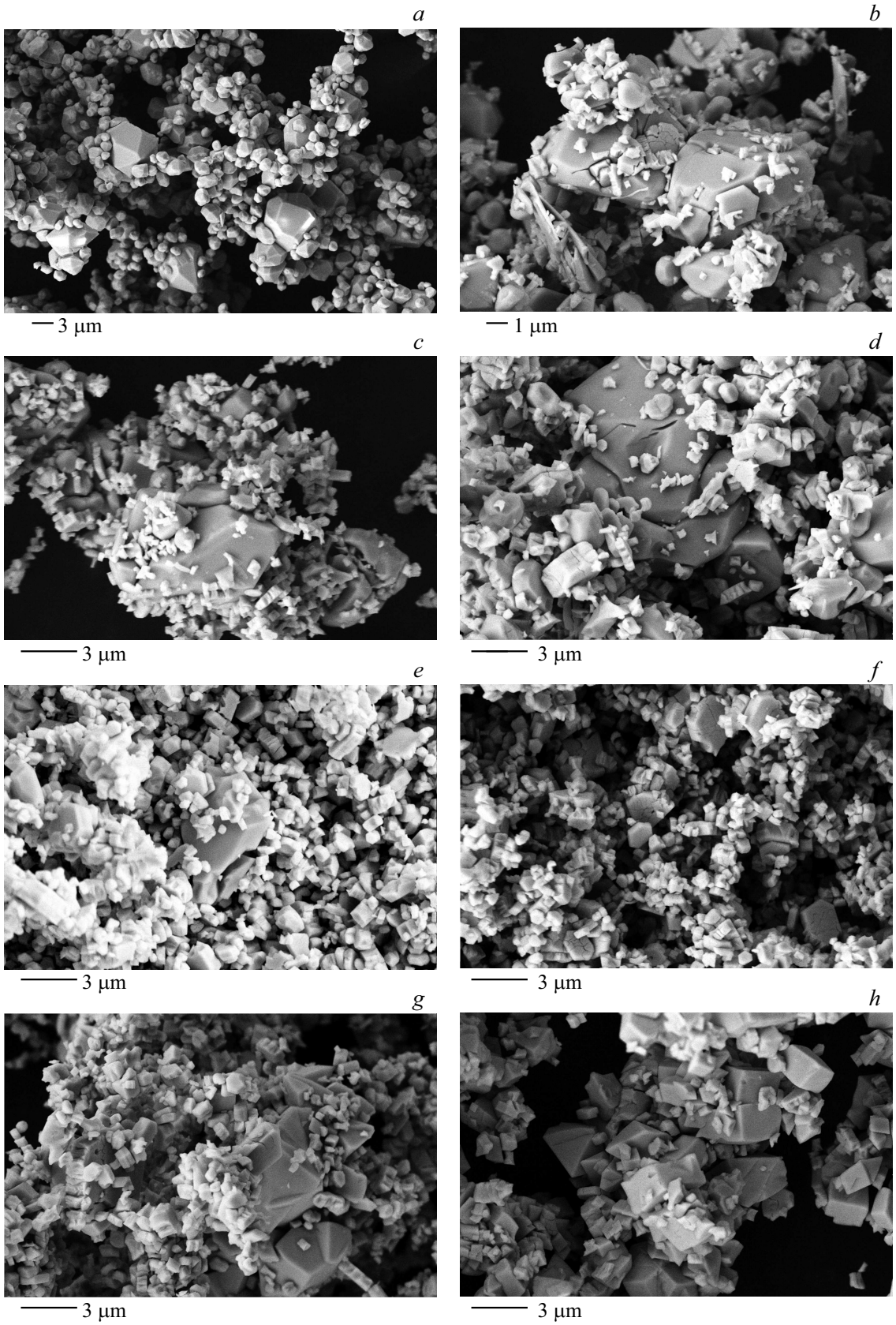

Figure 4. Morphology of the samples of $La_{0.98-x}Lu_xEu_{0.02}BO_3$. *a* — $La_{0.98}Eu_{0.02}BO_3$; *b* — $La_{0.78}Lu_{0.2}Eu_{0.02}BO_3$; *c* — $La_{0.68}Lu_{0.3}Eu_{0.02}BO_3$; *d* — $La_{0.48}Lu_{0.5}Eu_{0.02}BO_3$; *e* — $La_{0.25}Lu_{0.73}Eu_{0.02}BO_3$; *f* — $La_{0.1}Lu_{0.88}Eu_{0.02}BO_3$; *g* — $La_{0.075}Lu_{0.905}Eu_{0.02}BO_3$; *h* — $La_{0.063}Lu_{0.917}Eu_{0.02}BO_3$; *k* — $La_{0.05}Lu_{0.93}Eu_{0.02}BO_3$; *l* — $Lu_{0.98}Eu_{0.02}BO_3$.

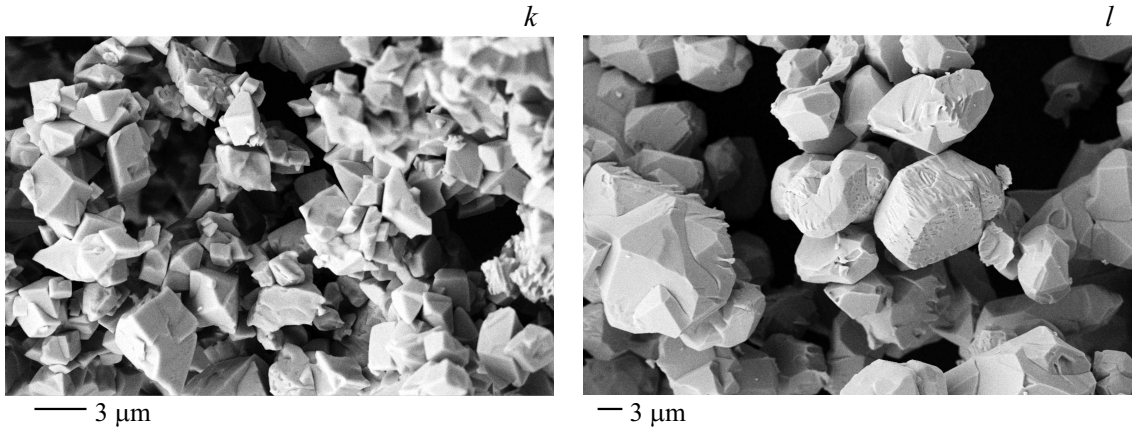

Fig. 4 (*cont.*).

Thus, the following conclusions can be made based on the X-ray diffraction studies of $La_{0.98-x}Lu_xEu_{0.02}BO_3$ compounds.

At $0 \le x < 0.15$ the samples are single-phase and have aragonite structure; at $0.15 \le x \le 0.8$ the samples are two-phase — they contain aragonite and vaterite phases; at $0.8 < x < 0.88$ vaterite is the dominant phase; at $0.88 \le x < 0.93$ the samples are two-phase and contain vaterite and calcite phases; at $0.93 \le x \le 0.98$ the samples have calcite structure.

The maximum possible dissolution of Lu^{3+} ions in the aragonite phase of $La_{0.98}Eu_{0.02}BO_3$ is ~ 13 at.%. The composition of the forming solid solution is $\sim La_{0.85}Lu_{0.13}Eu_{0.02}BO_3$.

The maximum possible dissolution of La^{3+} ions in the calcite phase of $Lu_{0.98}Eu_{0.02}BO_3$ is just ~ 5 at.%. The composition of the forming solid solution is $\sim La_{0.05}Lu_{0.93}Eu_{0.02}BO_3$. Such low value of La^{3+} limit solubility in the calcite phase of $Lu_{0.98}Eu_{0.02}BO_3$ is probably due to a large difference in the ionic radii of La^{3+} (1.115 Å) and Lu^{3+} (0.848 Å) [38].

4. Samples morphology

In samples of $La_{0.98-x}Lu_xEu_{0.02}BO_3$ in concentration range of Lu^{3+} $0 \le x \le 0.1$, that according to X-ray diffraction analysis data have aragonite structure (Table 1), the small (size of $\sim 1-2\,\mu$m) and large ($\sim 6-12\,\mu$m) microcrystals are observed (Fig. 4, *a*). At $0.3 \le x \le 0.8$ the sizes of small crystals reduce to $0.3-0.5\,\mu$m, and large crystals — to $3-6\,\mu$m. An increased concentration of Lu^{3+} ions leads to a decrease of aragonite amount and an increase of the vaterite amount (Table 1). With vaterite amount increase the number of small crystals increases ($0.3-0.5\,\mu$m) (Fig. 4, *b, c, d, e*). The samples of $La_{0.1}Lu_{0.88}Eu_{0.02}BO_3$, containing 98% of vaterite and 2% of calcite (Table 1), consist of microcrystals with size of 0.3–0.5 and $\sim 2\,\mu$m (Fig. 4, *f*). At $0.88 < x < 0.93$ the number of small microcrystals ($0.3-0.5\,\mu$m) decreases, while the number of microcrystals with size of $2-5\,\mu$m increases (Fig. 3, *g, h*). A decrease of the vaterite phase amount and an increase of the calcite phase share are observed in this range of Lu^{3+} ion concentrations (Table 1). The samples of $La_{0.05}Lu_{0.93}Eu_{0.02}BO_3$, containing 100% of calcite, have only microcrystals sized $3-5\,\mu$m (Fig. 4, *k*). $Lu_{0.98}Eu_{0.02}BO_3$ orthoborates, not containing La^{3+} ions, with a calcite structure (Table 1) consist of microcrystals sized $10-15\,\mu$m (Fig. 4, *l*). Thus, addition of a small number of La^{3+} ions (5 at.%) to $Lu_{0.98}Eu_{0.02}BO_3$ leads to a noticeable change of microcrystal sizes, but does not change the sample structure (Table 1).

The following conclusions can be made based on the morphology study of $La_{0.98-x}Lu_xEu_{0.02}BO_3$ at $0 \le x \le 0.98$. With the synthesis method used here, the samples, having an aragonite structure, consist of small ($\sim 1-2\,\mu$m) and large ($\sim 6-12\,\mu$m) microcrystals (Fig. 4, *a*). Orthoborates of $La_{0.1}Lu_{0.88}Eu_{0.02}BO_3$ (98% of vaterite, 2% of calcite) consist of small microcrystals sized 0.3–0.5 and $\sim 2\,\mu$m (Fig. 4, *f*), while the compounds of $Lu_{1-x}RE_xBO_3$ (RE = Eu, Gd, Tb), obtained using the same method and having vaterite structure, consist of microcrystals sized ($\sim 1-2\,\mu$m) [23,24]. The compounds of $La_{0.98-x}Lu_xEu_{0.02}BO_3$ ($0.93 \le x \le 0.98$) with a calcite structure consist of microcrystals, whose sizes at $x = 0.93$ and 0.98 are equal to 3–5 and $10-15\,\mu$m respectively (Fig. 4, *k, l*).

5. Results of IR-spectroscopy

Figure 5 shows IR-spectra of $La_{0.98-x}Lu_xEu_{0.02}BO_3$ compounds at $0 \le x \le 0.98$ in the frequency range of vibrations of B–O bonds. The spectrum for the sample of $La_{0.98}Eu_{0.02}BO_3$ composition (Fig. 5, spectrum *1*) contains absorption bands 592, 612, 721, 789, 939 and 1302 cm^{-1}. X-ray diffraction analysis showed, that this compound has a structure of the low-temperature aragonite $LaBO_3$ (Fig. 1, Table 1), which crystal structure contains flat trigonal groups of BO_3 [32].

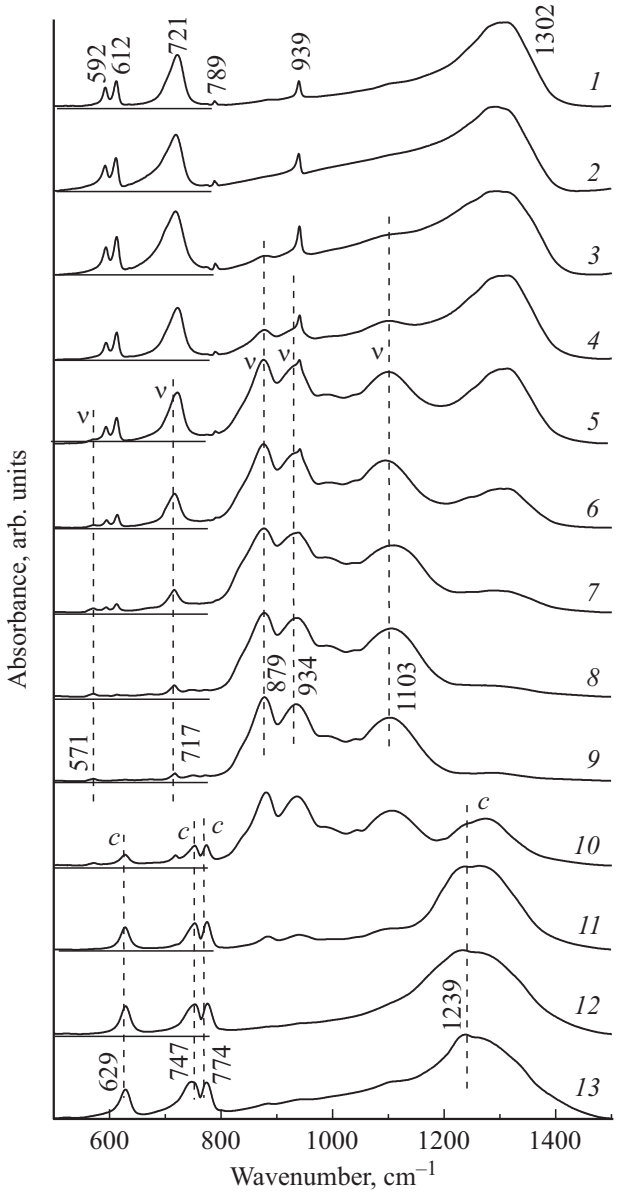

Figure 5. IR-spectra of $La_{0.98-x}Lu_xEu_{0.02}BO_3$ orthoborates. *1* — $La_{0.98}Eu_{0.02}BO_3$; *2* — $La_{0.88}Lu_{0.1}Eu_{0.02}BO_3$; *3* — $La_{0.83}Lu_{0.15}Eu_{0.02}BO_3$; *4* — $La_{0.78}Lu_{0.2}Eu_{0.02}BO_3$; *5* — $La_{0.68}Lu_{0.3}Eu_{0.02}BO_3$; *6* — $La_{0.48}Lu_{0.5}Eu_{0.02}BO_3$; *7* — $La_{0.35}Lu_{0.63}Eu_{0.02}BO_3$; *8* — $La_{0.18}Lu_{0.8}Eu_{0.02}BO_3$; *9* — $La_{0.10}Lu_{0.88}Eu_{0.02}BO_3$; *10* — $La_{0.075}Lu_{0.905}Eu_{0.02}BO_3$; *11* — $La_{0.063}Lu_{0.917}Eu_{0.02}BO_3$; *12* — $La_{0.05}Lu_{0.93}Eu_{0.02}BO_3$; *13* — $Lu_{0.98}Eu_{0.02}BO_3$. The zero values of ordinate axes for the spectra *1-12* are showed with a thin solid line.

Analysis of vibrations of planar $(BO_3)^{3-}$ ions in compounds with aragonite structure shows that 6 absorption bands, related to B–O bonds vibrations, should be observed in IR-spectra of these samples. Two bands of ν_3 and one band of ν_1 are stretching asymmetric and symmetric vibrations respectively, two bands of ν_4 and one of ν_2 are bending planar and out-of-plane vibrations respectively [35]. In spectra of $LaBO_3$ samples the splitting of the vibration band ν_3 is not observed, while doublet of the band ν_2 is explained by the presence of 2 boron isotopes in the samples — B^{10} and B^{11} [35,39]. Bands of IR-absorption 592 and 612 cm^{-1} are related to vibration of ν_4, doublet 721, 789 and absorption band 939 cm^{-1} — to ν_2 and ν_1 respectively, while band 1302 cm^{-1} — to vibration ν_3 (Fig. 5, spectrum *1*). Such IR-spectra of the samples with aragonite structure were observed in the works [35,39–41].

IR-spectrum of the sample of $La_{0.88}Lu_{0.1}Eu_{0.02}BO_3$ (Fig. 5, spectrum *2*), that has orthorhombic structure (Table 1), coincides with the spectrum of $La_{0.98-x}Eu_{0.02}BO_3$ (Fig. 5, spectrum *1*). With the further increase of Lu concentration in the spectra of $La_{0.98-x}Lu_xEu_{0.02}BO_3$ samples at $0.15 < x \leq 0.88$, along with aragonite absorption bands the additional bands appear („ν“, vertical dotted line) (Fig. 5, spectra *3–9*). Their intensity increases with increase of the Lu concentration, while intensity of the bands of the aragonite phase decreases. Since Lu is the alloying element, under conditions of the performed synthesis the formation of $LuBO_3$ orthoborate is possible. Lutetium orthoborate has two stable structural modifications: vaterite and calcite. In calcite phase the boron ions have trigonal coordination by oxygen $(BO_3)^{3-}$ [35]. In vaterite structure three boron-oxygen tetrahedrons form a group of $(B_3O_9)^{9-}$ as a three-dimensional ring [35,37].

Different surrounding of boron atoms is appeared in IR-spectra: the absorption band of stretching vibrations of B–O bonds in a vaterite structure is in the range of 800–1200 cm^{-1}, while in calcite structure its maximum is located near 1300 cm^{-1} [35,42,43]. The most intensive additional bands, observed in IR-spectra (Fig. 5, spectra *3–9*), are within a range of 800–1200 cm^{-1}. According to X-ray diffraction analysis data the samples of $La_{0.98-x}Lu_xEu_{0.02}BO_3$ at $0.15 < x \leq 0.8$ indeed contain aragonite and vaterite phases (Table 1). In spectra of samples of $La_{0.18}Lu_{0.8}Eu_{0.02}BO_3$ and $La_{0.1}Lu_{0.88}Eu_{0.02}BO_3$ (Fig. 5, spectra *8, 9*), in which vaterite is the dominant phase, the lines 571, 717, 879, 934 and 1103 cm^{-1} are observed. According to the results of X-ray diffraction analysis the vaterite has hexagonal structure (sp. gr. $P6_3/mmc$ № 194). In IR-spectra of $LuBO_3$(Tb) with a structure of vaterite with hexagonal symmetry of $P6_3/mmc$ [44,45] in frequency range of 800–1200 cm^{-1} three intensive bands, caused by stretching vibrations of B–O bonds of the ring and terminal bond of B–O were observed. In the samples, examined in this work, 3 intensive bands of 879, 934 and 1103 cm^{-1} are also observed (Fig. 5, spectra *8, 9*).

With increase of concentration of Lu^{3+} $(0.88 \leq x < 0.93)$ in IR-spectra of $La_{0.98-x}Lu_xEu_{0.02}BO_3$ compounds the additional bands („c“, vertical dotted line), characteristic for structure of calcite $LuBO_3$, appear along with vaterite absorption bands [13,35]. With increase of x the intensities of the bands, corresponding to vaterite structure, reduce, while of the bands „c“ — increase (Fig. 5, spectra *9–11*). These results correspond to X-ray diffraction analysis data, according to which the ratios of

Table 2. Maximums of the main bands in aragonite, vaterite and calcite luminescence excitation spectrum and their normalized intensities

Structure	Aragonite			Vaterite				Calcite			
λ_{ex}, nm	283	394	466.5	242	394	466.5	469	254	394	466.5	469
$^*I_{Eu}$	1	0.53	0.23	1	0.68	0.2	0.25	1	0.04	0.017	0.015

Note. $^*I_{Eu}$ — normalized intensities of the main bands in LES.

vaterite/calcite phases of the samples, that contain 88, 90.5 and 91.7 at.% of Lu^{3+} ions, are 98/2, 64/36 and 13/87% respectively (Table 1).

IR-spectra of $La_{0.05}Lu_{0.93}Eu_{0.02}BO_3$ and $Lu_{0.98}Eu_{0.02}BO_3$ samples, which have calcite structure (Table 1), are typical spectra of calcite phase (Fig. 5, spectra *12, 13*). Calcite structure, as well as aragonite structure, contains flat trigonal BO_3-groups. Absorption bands 629 and 747, 774 are caused by planar and out-of-plane bending vibrations of B–O bonds — ν_4 and ν_2, respectively, while the band with maximum of $\sim 1239\,cm^{-1}$ — by their valence asymmetric vibrations of ν_3 [13,35].

Thus, evolution of IR-spectra in the spectral range of B–O bonds vibrations showed, that with lutetium concentration increase in $La_{0.98-x}Lu_xEu_{0.02}BO_3$ samples the transition from aragonite structure, where boron has a trigonal coordination, to calcite structure, also having a trigonal coordination of boron, is happened through formation of vaterite phase, having tetrahedral coordination of boron. These results correspond to X-ray diffraction analysis data (Table 1, Fig. 2).

6. Luminescence spectra and luminescence excitation spectra

According to X-ray diffraction analysis data (section 3) in orthoborates of $La_{0.98-x}Lu_xEu_{0.02}BO_3$ with increase of x the sequential change of various types of crystal phases is observed: aragonite; aragonite and vaterite; vaterite; vaterite and calcite; calcite. Luminescence excitation spectra of the main luminescence bands and luminescence spectra of $La_{0.98-x}Lu_xEu_{0.02}BO_3$ compounds at $0 \le x \le 0.98$ are presented in Figs 6 and 7.

6.1. Luminescence excitation spectra

Excitation spectrum of the most intensive luminescence band of $La_{0.98}Eu_{0.02}BO_3$ orthoborate is presented in Fig. 6, spectrum *1*. The similar spectra are observed for samples of $La_{0.98-x}Lu_xEu_{0.02}BO_3$ at $0 \le x \le 0.3$. A wide band ($\lambda = 230-330$ nm) with maximum at ~ 283 nm (charge transfer band — CTB) is observed in excitation spectrum of the most intensive luminescence band of Eu^{3+} ions of orthoborate of $La_{0.98}Eu_{0.02}BO_3$ ($\lambda_{max} = 614.5$ nm ($^5D_0 \rightarrow {}^7F_2$)) in the ultraviolet spectral range. LES of $La_{0.98}Eu_{0.02}BO_3$ also contains several narrow bands in a wavelength range of 290–500 nm, corresponding to

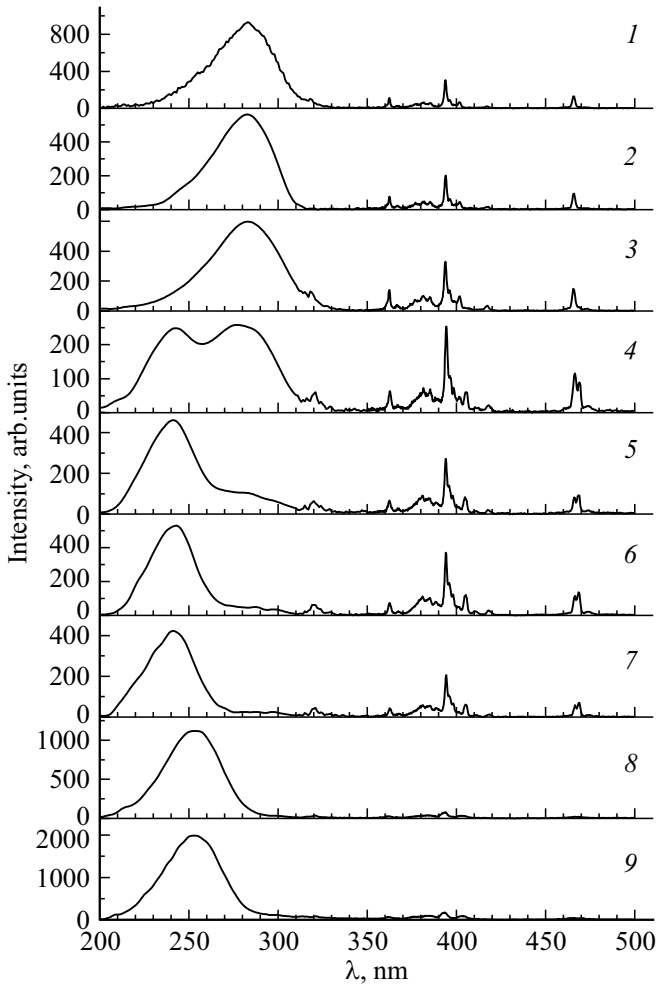

Figure 6. Luminescence excitation spectra for $La_{0.98-x}Lu_xEu_{0.02}BO_3$ orthoborates. *1* — $La_{0.98}Eu_{0.02}BO_3$; *2* — $La_{0.98}Eu_{0.02}BO_3$; *3* — $La_{0.68}Lu_{0.3}Eu_{0.02}BO_3$; *4* — $La_{0.48}Lu_{0.5}Eu_{0.02}BO_3$; *5* — $La_{0.25}Lu_{0.73}Eu_{0.02}BO_3$; *6* — $La_{0.18}Lu_{0.8}Eu_{0.02}BO_3$; *7* — $La_{0.1}Lu_{0.88}Eu_{0.02}BO_3$; *8* — $La_{0.063}Lu_{0.917}Eu_{0.02}BO_3$; *9* — $La_{0.05}Lu_{0.93}Eu_{0.02}BO_3$. *1, 3, 4* — $\lambda_{max} = 614.5$ nm; *2* — $\lambda_{max} = 589.$ nm; *5, 6* — $\lambda_{max} = 593.3$ nm; *7, 8* — $\lambda_{max} = 589.8$ nm.

resonance excitation of Eu^{3+} ions. The most intensive in the long-wave region of the spectrum are the bands, corresponding to resonance excitation of Eu^{3+} ions ($\lambda_{ex} = 394$ nm ($^7F_0 \rightarrow {}^5L_6$) and 466.5 nm ($^7F_0 \rightarrow {}^5D_2$)) (Fig. 6, spectrum *1*). Luminescence excitation spectrum of another one of the most intensive excitation bands of the samples of $La_{0.98}Eu_{0.02}BO_3$ ($\lambda_{max} = 589.5$ nm

($^5D_0 \rightarrow {}^7F_1$)) is presented in Fig. 6, spectrum *2*. It is identical to LES of the band with $\lambda_{max} = 614.5$ nm and contains CTB ($\lambda_{ex} \sim 283$ nm), as well as resonance bands $\lambda_{ex} = 394$ and 466.5 nm (Fig. 6, spectrum *2*). Moreover, the normalized intensities of the bands 283, 394, 466.5 nm for the spectra *1* and *2* (Fig. 6) are close, they are equal to 1, 0.32, 0.136 and 1, 0.3, 0.14 respectively. In LES of $La_{0.98-x}Lu_xEu_{0.02}BO_3$ orthoborates at $0 \le x \le 0.3$, as in the samples of $La_{0.98}Eu_{0.02}BO_3$, the narrow resonance bands $\lambda_{ex} \sim 394$ and 466.5 nm are observed, as well as the charge transfer band ($\lambda_{ex} \sim 283$ nm). As an example the LES of the $La_{0.68}Lu_{0.3}Eu_{0.02}BO_3$ sample is presented in Fig. 6, curve *3*. It should be noted, that with increase of Lu^{3+} concentration from 0 to 30 at.% the intensity of the bands 394 and 466.5 nm relating to CTB increases. For $La_{0.68}Lu_{0.3}Eu_{0.02}BO_3$ compound the normalized intensities of the bands 283, 394, 466.5 nm are equal to 1, 0.54, 0.245. According to the X-ray diffraction analysis data, an increased concentration of Lu^{3+} ions in $La_{0.98-x}Lu_xEu_{0.02}BO_3$ orthoborates leads to a decrease of aragonite phase and an increase of the vaterite phase (Table 1). The sample of $La_{0.68}Lu_{0.3}Eu_{0.02}BO_3$ contains 73% of aragonite (A) and 27% of vaterite (V). Drastic changes of luminescence excitation spectrum are observed in the sample of $La_{0.48}Lu_{0.5}Eu_{0.02}BO_3$ (55% of A and 45% of V) (Table 1). LES of this sample contains two short-wave bands $\lambda_{ex} \sim 242$ and 283 nm with almost the same intensity and resonance bands 394, 466.5 and 469 nm (Fig. 6, spectrum *4*). Band $\lambda_{ex} \sim 242$ nm corresponds to the charge transfer band in vaterite modification of $LuBO_3$(Eu).

With the further increase of Lu^{3+} ions concentration the intensity of the short-wave band $\lambda_{ex} \sim 283$ nm decreases, while in the samples, containing 80 at.% of Lu^{3+}, the band with $\lambda_{ex} \sim 242$ nm, as well as resonance bands 394, 466.5 and 469 nm (Fig. 6, spectra *5, 6*) are observed in luminescence excitation spectrum in ultraviolet spectral range. In LES of the $La_{0.18}Lu_{0.8}Eu_{0.02}BO_3$ samples, that contain 96% of V and 4% of A, the normalized intensities of the bands 283, 394, 466.5 nm are equal to 1, 0.68, 0.2 (Tables 1 and 2). The band with maximum at ~ 242 nm is also observed in luminescence excitation spectra of the $La_{0.98-x}Lu_xEu_{0.02}BO_3$ samples, with concentration of Lu^{3+} ions of 88 and 90.5 at.% (Fig. 6, spectrum *7*). In these samples, containing 98% of V, 2% of C and 64% of V, 36% of C (Table 1), the bands 394, 466.5 and 469 nm are also observed.

With the further increase of Lu^{3+} ions concentration the maximum of the charge transfer band is shifted to region of higher wavelengths (Fig. 6, spectra *8, 9*). For samples, alloyed with 91.7; 93 and 98 at.% of Lu^{3+} and containing 13% of V, 87% of C; 100% of C and 100% of C respectively (Table 1), CTB has maximum at ~ 254 nm. The normalized intensities of the bands 254, 394 and 466.5 nm for calcite modification are 1, 0.04 and 0.017, respectively (Table 2). The presented data indicate that with increase of calcite phase amount in LES the intensity of the short-wave band (CTB) with maximum at ~ 254 nm, intensity of which in calcite phase is $\sim 25-30$ times higher than the most intensive resonance band 394 nm, increases.

Table 2 contains maximums of the main bands in luminescence excitation spectrum (λ_{ex}) of the most intensive luminescence bands of various structural modifications of $La_{0.98-x}Lu_xEu_{0.02}BO_3$ compounds, as well as their normalized intensities. As seen from the table, there is no band with maximum at 469 nm in LES of aragonite, while maximums of the charge transfer bands for aragonite, vaterite and calcite phases are at wavelengths of 283, 242 and 254 nm respectively. It should also be noted, that in aragonite and vaterite structures the normalized intensities of the bands are close, while for calcite structure the intensity of the charge transfer band is significantly higher than of the resonance bands. The presence of the dominant short-wave band is an important feature of LES samples of $LuBO_3$ and $InBO_3$ with calcite structure.

6.2. Luminescence spectra

Luminescence spectra (LS) of $La_{0.98-x}Lu_xEu_{0.02}BO_3$ compounds ($x = 0$, 0.2. 0,3, 0.5, 0.88, 0.905, 0.917 and 0.98) in spectral range of $580-635$ nm at excitation with a light ($\lambda_{ex} = 394$ nm), corresponding to resonance excitation of Eu^{3+} ions, and in maximum of the charge transfer band ($\lambda_{ex} \sim 283-242$ nm), are presented in Fig. 7. Luminescence spectra of near-surface layer ($\lambda_{ex} = 283$ nm), and volume ($\lambda_{ex} = 394$ nm) of orthoborate of $La_{0.98}Eu_{0.02}BO_3$, that according to X-ray diffraction analysis data has aragonite structure (Table 1), coincide (Fig. 7, spectra *1* and *2*). They contain bands with $\lambda_{max} = 589.4$, 591 and 592.6 nm, corresponding to electron transfer $^5D_0 \rightarrow {}^7F_1$, as well as the bands 611.6, 614.5, 617.4, 619.8, 621.3 and 623 nm ($^5D_0 \rightarrow {}^7F_2$) (Fig. 8). At the same time in the luminescence spectrum (LS) of $LaBO_3$(Eu), studied in the works [29–31], one band is observed in a wavelength range of $589-593$ nm, and a wide band and a shoulder at a long-wave edge of this band are observed in a range of $610-623$ nm. Such difference in LS, obtained in this work and the works [29–31], is most likely due to the insufficiently high spectral resolution used in the registration of SL in these works.

Luminescence spectra of $La_{0.98-x}Lu_xEu_{0.02}BO_3$ compounds at $0 \le x < 0.15$, that have aragonite structure, according to X-ray diffraction analysis data (Table 1), are identical. In these samples the luminescence spectra of near-surface layer ($\lambda_{ex} = 283$ nm), and sample volume ($\lambda_{ex} = 394$ nm) coincide, as in the $La_{0.98}Eu_{0.02}BO_3$ sample (Fig. 7, spectra *1* and *2*).

In the $La_{0.78}Lu_{0.2}Eu_{0.02}BO_3$ samples, containing 89% of aragonite (A) and 11% of vaterite (V) (Table 1), the luminescence spectrum of near-surface layer ($\lambda_{ex} = 283$ nm) contains the bands, characteristic for aragonite structure of $LaBO_3$(Eu) (Fig. 7, spectrum *3*). At the same time, in luminescence spectrum of this sample volume ($\lambda_{ex} = 394$ nm), along with the bands, characteristic for

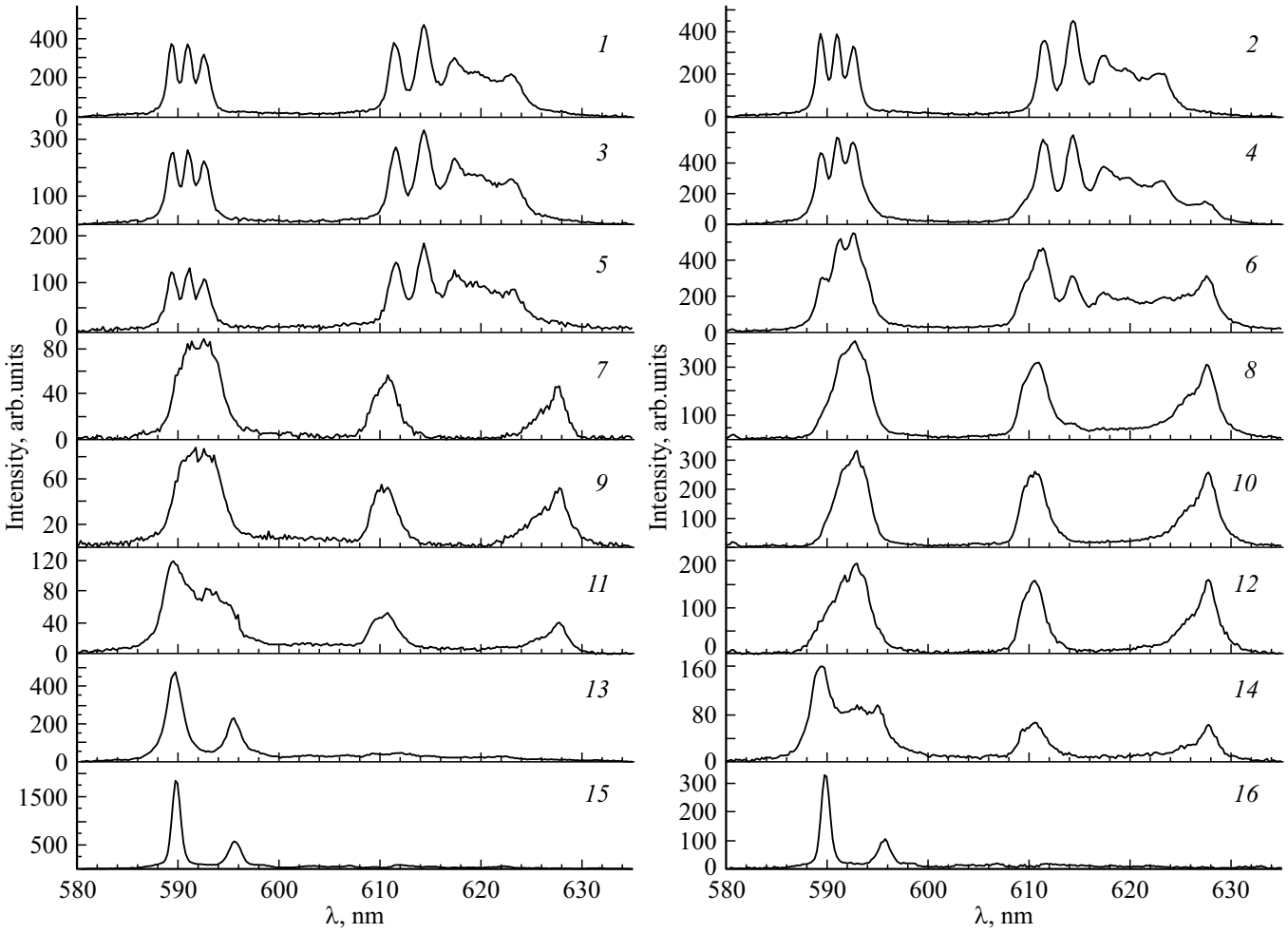

Figure 7. Luminescence spectra of $La_{0.98-x}Lu_xEu_{0.02}BO_3$ orthoborates. *1, 2* — $La_{0.98}Eu_{0.02}BO_3$; *3, 4* — $La_{0.78}Lu_{0.2}Eu_{0.02}BO_3$; *5, 6* — $La_{0.48}Lu_{0.5}Eu_{0.02}BO_3$; *7, 8* — $La_{0.25}Lu_{0.73}Eu_{0.02}BO_3$; *9, 10* — $La_{0.1}Lu_{0.88}Eu_{0.02}BO_3$; *11, 12* — $La_{0.075}Lu_{0.905}Eu_{0.02}BO_3$; *13, 14* — $La_{0.063}Lu_{0.917}Eu_{0.02}BO_3$; *15, 16* — $Lu_{0.98}Eu_{0.02}BO_3$. *1, 3, 5* and *7* — $\lambda_{ex} = 283$ nm; *9* and *11* — $\lambda_{ex} = 242$ nm; *13* and *15* — $\lambda_{ex} = 254$ nm; *2, 4, 6, 8, 10, 12, 14* and *16* — $\lambda_{ex} = 394$ nm.

aragonite structure, the band ($\lambda_{max} \sim 628$ nm) appears, corresponding to vaterite structure of $LuBO_3$(Eu). Besides, the changes appear in ratio of intensities of the bands with $\lambda_{max} = 589.4$, 591 and 592.6 nm (Fig. 7, spectrum *4*). Thus, the formation of vaterite phase happens in a volume of microcrystals with aragonite structure. Bigger changes in LS of the sample volume ($\lambda_{ex} = 394$ nm) are observed in compounds of $La_{0.68}Lu_{0.3}Eu_{0.02}BO_3$ (73% of A, 26% of V) and $La_{0.48}Lu_{0.5}Eu_{0.02}BO_3$ (55% of A, 45% of V). In these samples the intensity of the band ~ 628 nm increases, and changes in the wavelength region of 598–596 nm are observed (Fig. 7, curve *6*). At the same time, in luminescence spectrum of near-surface layer ($\lambda_{ex} = 283$ nm) only the bands, characteristic for aragonite structure, are observed (Fig. 7, spectrum *5*). As noted, in luminescence excitation spectrum of the $La_{0.48}Lu_{0.5}Eu_{0.02}BO_3$ samples two bands with maximums of 242 and 283 nm are observed in the ultraviolet spectral range (Fig. 6, spectrum *4*). Short-wave band $\lambda_{ex} = 242$ nm corresponds to CTB in vaterite modification of $LuBO_3$(Eu). It is important to note, that LS of near-surface layer of $La_{0.48}Lu_{0.5}Eu_{0.02}BO_3$ at excitation with a light with $\lambda_{ex} = 242$ nm contains the bands, characteristic for vaterite modification (Fig. 9). As noted, with the further increase of Lu^{3+} ions concentration in the short-wave spectral range of the luminescence excitation the significant increase of intensity of the band with $\lambda_{ex} = 242$ nm is observed (Fig. 6, spectrum *5*). In these samples the bands, characteristic for vaterite phase, are observed not only in LS of the volume, but also in near-surface layers of the sample. In luminescence spectra of near-surface layer ($\lambda_{ex} = 242$ nm) and volume ($\lambda_{ex} = 394$ nm) of orthoborates of $La_{0.35}Lu_{0.63}Eu_{0.02}BO_3$ (29% of A and 71% of V), $La_{0.25}Lu_{0.73}Eu_{0.02}BO_3$ (20% of A and 80% of V) and $La_{0.18}Lu_{0.8}Eu_{0.02}BO_3$ (4% of A and 96% of V) the bands, characteristic for vaterite modification of $LuBO_3$(Eu) compounds are observed (Fig. 7, spectra *7, 8*).

According to X-ray diffraction analysis data (Table 1) in orthoborates of $La_{0.98-x}Lu_xEu_{0.02}BO_3$ at $0.84 < x \leq 0.98$

the sequential change of 3 types of structural modifications is observed. Initially the ortoborates have vaterite structure, then they become two-phase — calcite phase appears along with vaterite structure. At $0.93 < x \leq 0.98$ the whole sample volume has calcite structure (C) (Table 1). Luminescence spectra of near-surface layer ($\lambda_{ex} = 242$ nm), and volume ($\lambda_{ex} = 394$ nm) of the $La_{0.1}Lu_{0.88}Eu_{0.02}BO_3$ compound (98% of V and 2% of C) contain bands, characteristic for vaterite structure of $LuBO_3$(Eu) orthoborate (Fig. 7, spectra *9, 10*). With increase of Lu^{3+} ions concentration the amount of calcite phase increases and luminescence spectrum of near-surface layer of the $La_{0.075}Lu_{0.905}Eu_{0.02}BO_3$ sample (64% of V, 34% of C) contains bands $\lambda_{max} = 589.8$ and 595.7 nm, characteristic for calcite modification of $LuBO_3$(Eu) (Fig. 7, spectrum *11*). At the same time, LS of volume of this sample contains only the bands, characteristic for vaterite structure of $LuBO_3$(Eu) (Fig. 7, spectrum *12*). Thus, formation of calcite phase in samples with vaterite structure happens in near-surface sample layer. The further increase of Lu^{3+} concentration results in formation of the bands, characteristic for calcite modification, in LS of sample volume. Luminescence spectrum of volume of $La_{0.063}Lu_{0.917}Eu_{0.02}BO_3$ (13% of V, 87% of C) contains bands, characteristic for vaterite and calcite structures (Fig. 7, spectrum *14*). At the same time, LS of near-surface layer of this sample contains only the bands of calcite phase of $LuBO_3$(Eu) (Fig. 7, spectrum *13*). Luminescence spectra of near-surface layer and volume of $La_{0.05}Lu_{0.93}Eu_{0.02}BO_3$ and $Lu_{0.98}Eu_{0.02}BO_3$ compounds, that have calcite structure (Table 1), contain only the bands of calcite modification of $LuBO_3$(Eu) (Fig. 7, spectra *15, 16*).

Based on comparison of X-ray diffraction analysis and spectral studies results the conclusion can be made on correspondence of structure and spectral characteristics of orthoborates of $La_{0.98-x}Lu_xEu_{0.02}BO_3$. Increase of x results in sequential change of various structural modifications. At $0 \leq x < 0.15$ the compound has aragonite structure and the bands, corresponding to aragonite structure, are observed in LS (Fig. 7, spectra *1, 2*). At $0.15 \leq x \leq 0.84$ the samples are two-phase, they contain aragonite and vaterite phases, and LS of these samples contains the bands of aragonite and vaterite modifications (Fig. 7, spectra *3–8*). At $0.8 < x < 0.88$ orthoborates have vaterite structure and LS contains the bands of vaterite modification (Fig. 7, spectra *9, 10*). At $0.88 < x < 0.93$ the phases of vaterite and calcite are observed and LS contains the bands, corresponding to vaterite and calcite structures (Fig. 7, spectra *11–14*). At $0.93 \leq x \leq 0.98$ the samples have calcite structure, and LS contains the bands of calcite phase of $LuBO_3$(Eu) (Fig. 7, spectra *15, 16*).

It is important to note, that with increase of Lu^{3+} ions concentration the vaterite phase is formed in the volume of samples of $La_{0.98-x}Lu_xEu_{0.02}BO_3$ with aragonite structure. With the further increase of Lu^{3+} ions concentration the vaterite phase is also formed on the sample surface. This process is similar to formation of vaterite phase in the volume of large microcrystals of $Lu_{0.99-x}RE_xEu_{0.01}BO_3$ (where RE = Gd, Eu, Tb, Y) with calcite structure [23,24].

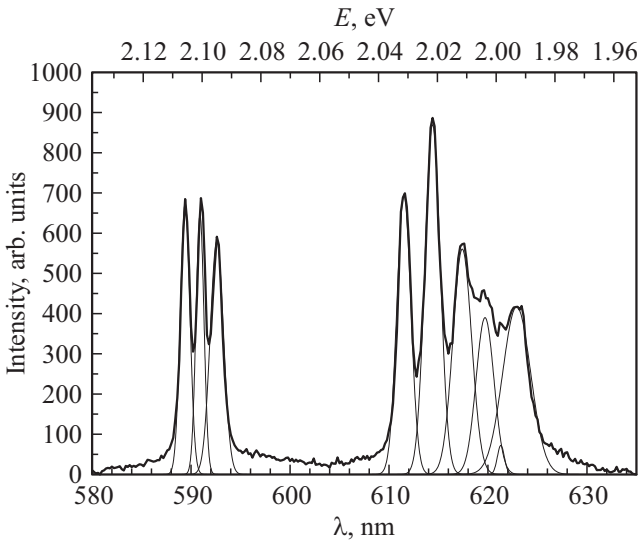

Figure 8. Decomposition of the bands 588–596 and 610–635 nm (Fig. 7, spectrum *2*) into components. At spectrum decomposition an energy scale was used, after spectrum decomposition the transition from eV to nm was performed.

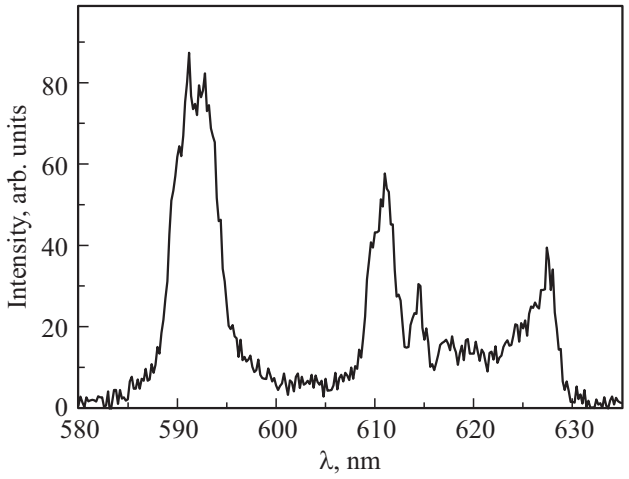

Figure 9. Luminescence spectrum of orthoborate of $La_{0.48}Lu_{0.5}Eu_{0.02}BO_3$ at excitation with a light with $\lambda_{ex} = 242$ nm.

At the same time, formation of calcite at $0.88 < x < 0.93$ in $La_{0.98-x}Lu_xEu_{0.02}BO_3$ orthoborates with the vaterite structure happens in the near-surface regions of the sample, like in the compounds of $Lu_{0.98-x}In_xEu_{0.02}BO_3$ [22].

Figure 10 shows the dependencies of the normalized integral luminescence intensities (areas below luminescence curves) of $La_{0.98-x}Lu_xEu_{0.02}BO_3$ orthoborates in a range of 2.138–1.953 eV (580–635 nm) on Lu ions concentration ($0 \leq x \leq 0.98$) at excitation in the maximum of the charge transfer band ($\lambda_{ex} \sim 283–242$ nm) (S_{CTB}) and resonance excitation of Eu^{3+} ions ($\lambda_{ex} = 394$ nm) (S_{394}). The integral luminescence intensity at excitation in CTB (Fig. 10,

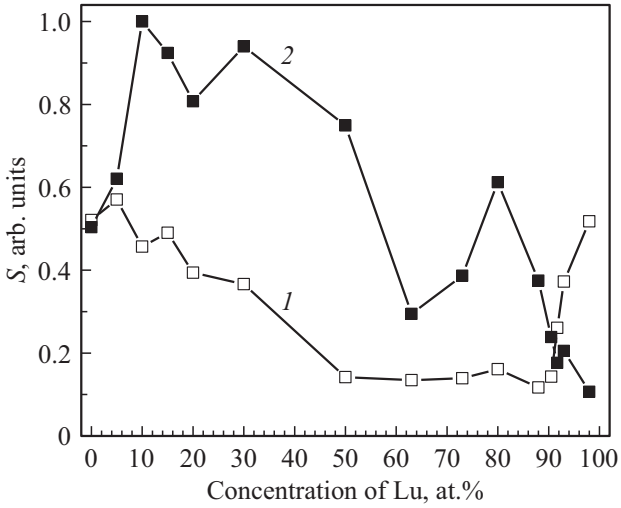

Figure 10. Dependencies of integral luminescence intensity on Lu ions concentration — S (areas below luminescence curves) for $La_{0.98-x}Lu_xEu_{0.02}BO_3$ orthoborates in a range of 2.138−1.953 eV (580−635 nm). *1* — at excitation in the maximum of the charge transfer band (CTB) — S_{CTB} ($\lambda_{ex} \sim 283-242$ nm); *2* — at excitation with a light of $\lambda_{ex} = 394$ nm — S_{394}.

curve *1*) at increase of Lu concentration ($0 \le x < 0.5$) reduces, in a range of $0.5 \le x \le 0.905$ S_{CTB} it remains almost the same, and at $0.905 < x \le 0.98$ CTB increase is observed. Integral luminescence intensities at excitation in the charge transfer band at $0 \le x \le 0.1$ and $x = 0.98$ are close.

Integral luminescence intensity at resonance excitation of Eu^{3+} ions in $La_{0.98-x}Lu_xEu_{0.02}BO_3$ compound (S_{394}) increases at Lu concentration growth, reaching the maximum value at $x = 0.1$, and then decreases. At $x = 0.8$ the second maximum is observed on the dependence of S_{394} of lutetium concentration (Fig. 10, curve *2*). It should be noted, that the maximum value of S_{394} exceeds the value of S_{394} at $x = 0$ by a factor of 2.

As known, electron transitions between the states of free ions of Eu^{3+}, pertaining to one configuration, in our case the $4f^n$-configuration, are prohibited by parity [14,15]. Under crystal field exposure this prohibition is partly lifted. At displacement of La^{3+} ions with ionic radius of 1.114 Å, with Lu^{3+} ions, having significantly less ionic radius (0.867 Å) [38], the value of crystal field in $La_{0.98-x}Lu_xEu_{0.02}BO_3$ increases, resulting in increase of luminescence intensity of Eu^{3+} at resonance excitation (Fig. 10, curve *2*).

It is important to note, that for $La_{0.98-x}Lu_xEu_{0.02}BO_3$ samples, having the aragonite structure (Table 1) at $0 \le x < 0.15$, the maximum of integral luminescence intensity at resonance excitation of Eu^{3+} ions ($\lambda_{ex} = 394$ nm) (S_{394}) is observed at $x = 0.1$. This indicates, that increase of S_{394} at $x = 0.1$ is not related to structural transformations, but is defined by a change of Lu^{3+} ions concentration in aragonite modification of $La_{0.98-x}Lu_xEu_{0.02}BO_3$.

Let's examine the solid solution of $Lu_{0.98-y}La_yEu_{0.02}BO_3$. This compound, according to abovementioned data, has the calcite structure at $0 \le y \le 0.05$. At $0.05 < y \le 0.1$ the compound is two-phase — contains calcite and vaterite phases, and at $0.1 < y < 0.18$ it has vaterite structure (Table 1). Since compounds of $LuBO_3$ and $LaBO_3$, synthesized at 970°C, have calcite and aragonite structure respectively [12,1,25], one could expect, that in the compounds of $Lu_{0.98-y}La_yEu_{0.02}BO_3$, synthesized at 970°C, increase of y will result in gradual decrease of calcite phase amount and increase of aragonite phase. However the presented experimental data on studies of phase formation in $Lu_{0.98-y}La_yEu_{0.02}BO_3$ compounds do not confirm this assumption. With increase of La^{3+} concentration, the formation of the vaterite phase occurs, that is, in a solid solution of $Lu_{0.98-y}La_yEu_{0.02}BO_3$ at $0 \le y \le 0.1$, La^{3+} ions play the same phase-forming role as RE^{3+} ions (RE = Eu, Gd, Tb, Y) in the orthoborate $Lu_{0.98-y}RE_yEu_{0.02}BO_3$.

Different impact on phase formation of $Lu_{0.98-y}RE_yEu_{0.02}BO_3$ of La^{3+} and RE^{3+} ions appears at $0.18 < y \le 0.98$. In this range of y concentrations the $Lu_{0.98-y}RE_yEu_{0.02}BO_3$ compound has vaterite structure, while in $Lu_{0.98-y}La_yEu_{0.02}BO_3$ orthoborate at increase of y the decrease of vaterite phase amount and increase of aragonite phase are observed.

One could assume, that presence of 2 at.% of Eu^{3+} ions in $Lu_{0.98-y}La_yEu_{0.02}BO_3$ orthoborate, which are used as optically active and structure-sensitive markers, results in formation of vaterite phase at $0.05 \le y \le 0.1$. Would this assumption be true, the compound of $Lu_{0.9}La_{0.1}BO_3$ should also have aragonite structure. However, according to X-ray diffraction analysis data, the $Lu_{0.9}La_{0.1}BO_3$ sample contains 93% of vaterite and 7% of calcite, while $Lu_{0.88}La_{0.1}Eu_{0.02}BO_3$ sample contains 98% of vaterite and 2% of calcite (Table 1). This data indicate that presence of 2 at.% of Eu^{3+} ions in $Lu_{0.98-y}La_yEu_{0.02}BO_3$ orthoborate does not significantly influence on formation of structural state in these compounds.

7. Conclusion

In this work the studies of structure, morphology, IR-spectra and spectra of luminescence excitation and luminescence of near-surface layer and volume of $La_{0.98-x}Lu_xEu_{0.02}BO_3$ orthoborates at $0 \le x \le 0.98$, synthesized at 970°C, were performed.

The univalent correspondence of structural modification and spectral characteristics of photoluminescence and IR-spectra of orthoborates is established. The study of luminescence spectra at various wavelengths of excitation light allowed to obtain information on structure of near-surface layer and volume of the examined samples.

It is shown, that in $La_{0.98-x}Lu_xEu_{0.02}BO_3$ orthoborates the increase of Lu^{3+} ions concentration results in sequential change of their structural state and spectral characteristics.

– At $0 \le x \le 0.1$ the compounds are single-phase and have an aragonite structure (sp.gr. $Pnam$). Luminescence spectra of Eu^{3+} ions in near-surface layer and volume of microcrystals of these samples, corresponding to aragonite structure, contain the bands with $\lambda_{max} = 589.4$, 591 and 592.6 nm, corresponding to electron transition $^5D_0 \rightarrow {}^7F_1$, as well as the bands 611.6, 614.5, 617.4, 619.8, 621.3 and 623 nm ($^5D_0 \rightarrow {}^7F_2$). The IR-spectra have the absorption bands 592, 612, 721, 789, 939 and 1302 cm^{-1}, which correspond to the aragonite phase.

– At $0.15 \le x \le 0.8$ the samples of $La_{0.98-x}Lu_xEu_{0.02}BO_3$ are two-phase, they contain aragonite and vaterite phases, luminescence spectra and IR-spectra contain the bands, characteristic to aragonite structures of $La_{0.98}Eu_{0.02}BO_3$ and vaterite of $LuBO_3$(Eu).

– At $0.8 < x < 0.88$ the orthoborates have a vaterite structure (sp.gr. $P6_3/mmc$). Luminescence spectra of Eu^{3+} ions in near-surface layer and volume of microcrystals of these samples are identical and contain the bands 588−596, 608−613 and 624−632 nm, characteristic for vaterite modification of $LuBO_3$(Eu). In IR-spectra of vaterite phase the absorption bands 571, 717, 879, 934 and 1103 cm^{-1} are observed.

– At $0.88 < x < 0.93$ the samples of $La_{0.98-x}Lu_xEu_{0.02}BO_3$ are two-phase, they contain vaterite and calcite phases, luminescence spectra and IR-spectra contain the bands, characteristic to vaterite and calcite modifications of these samples.

– At $0.93 \le x \le 0.98$ the orthoborates are single-phase and have a calcite structure (sp.gr. $R\bar{3}c$). Luminescence spectra and IR-spectra have the bands, characteristic for calcite modification of $LuBO_3$(Eu). Luminescence spectra of near-surface layer and volume of microcrystals of these samples contain 2 narrow bands with $\lambda_{max} = 589.8$ and 595.7 nm ($^5D_0 \rightarrow {}^7F_1$), and IR-spectra contain the absorption bands 629, 747, 774 and 1239 cm^{-1}.

It is established, that with increase of x the formation of vaterite phase in the $La_{0.98-x}Lu_xEu_{0.02}BO_3$ samples, initially with aragonite structure, happens in the samples volume at first. The further increase of Lu^{3+} ions concentration results in formation of vaterite structure in the entire sample.

At the same time, a calcite phase (at $0.88 < x < 0.93$) in $La_{0.98-x}Lu_xEu_{0.02}BO_3$ orthoborates with the vaterite structure forms in the sample near-surface regions first, and then a calcite structure forms in the entire sample.

Orthoborates of $La_{0.98-x}Lu_xEu_{0.02}BO_3$ have high luminescence intensity and can be used as an efficient red luminophores for LED light sources.

Acknowledgments

The authors would like to thank the Research Facility Center of ISSP of RAS for the morphology study of the samples and their characterization by IR-spectroscopy and X-ray diffraction analysis methods.

Funding

The work has been performed under the state assignment of ISSP of RAS.

Conflict of interest

The authors declare that they have no conflict of interest.

References

[1] C. Mansuy, J.M. Nedelec, C. Dujardin, R. Mahiou. Opt. Mater. **29**, *6*, 697 (2007).
[2] G. Blasse, B.C. Grabmaier. Luminescent Materials. Springer–Verlag, Berlin–Heiderberg (1994). 233 p.
[3] Jun Yang, Chunxia Li, Xiaoming Zhang, Zewei Quan, Cuimiao Zhang, Huaiyong Li, Jun Lin. Chem. Eur. J. **14**, *14*, 4336 (2008).
[4] Y.H. Zhou, J. Lin, S.B. Wang, H.J. Zhang. Opt. Mater. **20**, *1*, 13 (2002).
[5] J. Yang, G. Zhang, L. Wang, Z. You, S. Huang, H. Lian, J. Lin. J. Solid State Chem. **181**, *12*, 2672 (2008).
[6] S.Z. Shmurak, A.P. Kiselev, V.V. Sinitsyn, I.M. Shmyt'ko, A.S. Aronin, B.S. Red'kin, E.G. Ponyatovsky. FTT **48**, *1*, 48 (2006) (in Russian).
[7] S.Z. Shmurak, A.P. Kiselev, N.V. Klassen, V.V. Sinitsyn, I.M. Shmyt'ko, B.S. Red'kin, S.S. Khasanov. IEEE Trans. Nucl. Sci. **55**, *1−3*, 1128 (2008).
[8] S.Z. Shmurak, A.P. Kiselev, D.M. Kurmasheva, B.S. Red'kin, V.V. Sinitsyn. ZhETF **137**, *5*, 867 (2010) (in Russian).
[9] S.Z. Shmurak, V.V. Kedrov, A.P. Kiselev, I.I. Zver'kova. FTT **55**, *2*, 336 (2013) (in Russian).
[10] S.Z. Shmurak, V.V. Kedrov, A.P. Kiselev, T.N. Fursova, I.M. Shmyt'ko. FTT **58**, *3*, 564 (2016) (in Russian).
[11] A.A. Mazilkin, O.G. Rybchenko, T.N. Fursova, S.Z. Shmurak, V.V. Kedrov. Mater. Character. **147**, 215 (2019).
[12] S.Z. Shmurak, V.V. Kedrov, A.P. Kiselev, I.M. Shmyt'ko. FTT **57**, *1*, 19 (2015) (in Russian).
[13] S.Z. Shmurak, V.V. Kedrov, A.P. Kiselev, T.N. Fursova, I.M. Shmyt'ko. FTT **57**, *8*, 1558 (2015) (in Russian).
[14] M.A. Elyashevich. Spektroskopiya redkikh zemel'. GITTL, M. (1953). 456 p. (in Russian).
[15] M.I. Gaiduk, V.F. Zolin, L.S. Gaigerova. Spektry lyuminestsentsii evropiya. Nauka, M. (1974). 195 p. (in Russian).
[16] J. Hölsä. Inorg. Chim. Acta **139**, *1−2*, 257 (1987).
[17] E.M. Levin, R.S. Roth, J.B. Martin. Am. Miner. **46**, *9−10*, 1030 (1961).
[18] G. Chadeyron, M. El-Ghozzi, R. Mahiou, A. Arbus, C. Cousseins. J. Solid State Chem. **128**, 261 (1997).
[19] D. Santamaría-Pérez, O. Gomis, J. Angel Sans, H.M. Ortiz, A. Vegas, D. Errandonea, J. Ruiz-Fuertes, D. Martinez-Garcia, B. Garcia-Domene, André L.J. Pereira, F. Javier Manjón, P. Rodríguez-Hernández, A. Muñoz, F. Piccinelli, M. Bettinelli, C. Popescu. J. Phys. Chem. C **118**, 4354 (2014).
[20] Wen Ding, Pan Liang, Zhi-Hong Liu. Mater. Res. Bull. **94**, 31 (2017).
[21] WenDing, Pan Liang, Zhi-Hong Liu. Solid State Sci. **67**, 76 (2017).
[22] S.Z. Shmurak, V.V. Kedrov, A.P. Kiselev, T.N. Fursova, I.I. Zver'kova. FTT **62**, *12*, 2110 (2020).(in Russian).

[23] S.Z. Shmurak, V.V. Kedrov, A.P. Kiselev, T.N. Fursova, I.I. Zver'kova, E.Yu. Postnova. FTT **63**, *7*, 933 (2021) (in Russian).
[24] S.Z. Shmurak, V.V. Kedrov, A.P. Kiselev, T.N. Fursova, I.I. Zver'kova, E.Yu. Postnova. FTT **63**, *10*, 1615 (2021) (in Russian).
[25] R.S. Roth, J.L. Waring, E.M. Levin, Proc. 3rd Conf. Rare Earth Res. Clearwater, Fla. (1964). P. 153.
[26] C. Badan, O. Esenturk, A. Yelmaz. Solid State Sci., **14**, *11–12*, 1710 (2012).
[27] I.M. Shmyt'ko, I.N. Kiryakin, G.K. Strukova. FTT **55**, *7*, 1369 (2013) (in Russian).
[28] A.P. Kiselev, S.Z. Shmurak, B.S. Red'kin, V.V. Sinitsyn, I.M. Shmyt'ko, E.A. Kudrenko, E.G. Ponyatovsky. FTT **48**, *8*, 1458 (2006) (in Russian).
[29] N.I. Steblevskaya, M.I. Belobeletskaya, M.A. Medkov. Zhurn. neorgan. khimii **66**, *4*, 440 (2021) (in Russian).
[30] J. Guang, C. Zhang, C. Wang, L. Liu, C. Huang, S. Ding. Cryst. Eng. Commun. **14**, 579 (2012).
[31] J. Zhang, M. Yang, H. Jin, X. Wang, X. Zhao, X. Liu, L. Peng. Mater. Res. Bull. **47**, 247 (2012).
[32] Heng-Wei Wei, Li-Ming Shao, Huan Jiao, Xi-Ping Jing. Opt. Mater. **75**, 442 (2018).
[33] R. Nayar, S. Tamboli, A.K. Sahu, V. Nayar, S.J. Dhoble. J. Fluoresc. **27**, 251 (2017).
[34] S.K. Omanwar, N.S. Savala. Appl. Phys. A **123**, 673 (2017).
[35] C.E. Weir, E.R. Lippincott. J. Res. Natl. Bur. Std.-A. Phys. Chem. **65A**, *3*, 173 (1961).
[36] A. Szczeszak, T. Grzyb, St. Lis, R.J. Wiglusz. Dalton Transact. **41**, 5824 (2012).
[37] Ling Li, Shihong Zhou, Siyuan Zhang. Solid State Sci. **10**, 1173 (2008).
[38] A.G. Ryabukhin. Izv. Chelyabinskogo nauch. tsentra **4**, 33 (2000) (in Russian).
[39] W.C. Steele, J.C. Decius. J. Chem. Phys. **25**, *6*, 1184 (1956).
[40] Radha Velchuri, B. Vijaya Kumar, V. Rama Devi, G. Prasad, D. Jaya Prakash, M. Vithal. Mater. Res. Bull. **46**, 1219 (2011).
[41] Cansin Badan, Okan Esenturk, Ayşen-Yılmaz. Solid State Sci. **14**, 1710 (2012).
[42] D. Boyer, F. Leroux, G. Bertrand, R. Mahiou. J. Non-Crystalline Solids **306**, 110 (2002).
[43] J.P. Laperches, P. Tarte. Spectrochim. Acta **22**, 1201 (1966).
[44] Jun Yang, Cuimiao Zhang, Lili Wang, Zhiyao Hou, Shanshan Huang, Hongzhou Lian, Jun Lin. J. Solid State Chem. **181**, 2672 (2008).
[45] S.Z. Shmurak, V.V. Kedrov, A.P. Kiselev, T.N. Fursova, O.G. Rybchenko. FTT **59**, *1*, 1150 (2017) (in Russian).